

# MÖSSBAUER INVESTIGATION OF STATIC-DISORDER CRYSTALLINE MEDIA. III. DISPERSION OF ELECTRIC AND MAGNETIC HYPERFINE FIELDS IN STATIC-DISORDER CRYSTALLINE MEDIA

S. CONSTANTINESCU

*National Institute of Materials Physics, P.O. Box MG-07, Bucharest, Romania*

(Received May 10, 2004)

*Abstract.* A careful analysis evidenced the dispersion of the electric and hyperfine magnetic fields in the  $^{57}\text{Fe}$  Mössbauer spectra on some static-disordered crystalline media with melilite and Ca-gallate structure. A detailed discussion is done about the causes generating the distribution of crystalline fields in such media.

*Key words:* Mössbauer effect, crystal structure, static disorder, electric hyperfine fields, field dispersion.

## 1. INTRODUCTION

In the last ten years a special attention was paid to the class of static-disordered crystalline media for their interesting properties of scientific as well as of practical importance. These media are obtained by changing the chemical composition across the crystalline medium. So, the crystallographic nonequivalence of ions occupying sites with slightly different crystal-field is given by the statistical distribution of more than a single sort of ions over similar lattice sites. The effect of this change is reflected in variations of all the crystal parameters, but especially in the occupancy and the electric and/or magnetic local fields of different crystallographic sites. Due to the narrow line-width of the  $\gamma$ -resonances, the Mössbauer technique (designated by the abbreviations MS or NGR) can detect any changes and slight differences of the electric and/or magnetic hyperfine interactions, by the hyperfine spectral parameter [1].

The aim of this work is to present and to analyze the crystal field dispersion, which was detected by MS in the new compounds of tetragonal and trigonal ferrigehlenites and ferric- and trivalent lanthanide-gallates, in order to make a model of crystal field dispersion in such media. These new compounds have the melilite structure,  $\text{A}_2\text{Fe}_2\text{ZO}_7$  ( $\text{A} = \text{Ba}, \text{Sr}$ ;  $\text{Z} = \text{Ge}, \text{Si}$ ; space group  $P\bar{4}2_1m$ ), and,

respectively, the Ca-gallate structure,  $A_{3-y}Ln_yFe_{2+y}Ge_{4-y}O_{14}$  ( $Ln = La, Nd$ ; space group  $P3, P321$ ).

Generally, the random occupation of one or more lattice sites by different ionic sorts without the polyhedral changes with their concentration will induce the crystal field dispersion. So in the above mentioned structures, the ions  $A^{2+}/Ln^{3+}$  and  $Fe^{3+}/Ge^{4+}$  enter into Thompson cubes and, respectively, Oh (octahedral) and/or T (tetrahedral) sites, [2, 3].

These compounds were chosen due to their practical importance. Such disordered crystalline media are the host matrices for tunable laser activator ions, piezoelectric crystals with attractive electromechanical coupling factor and materials having special magnetic properties depending on the doping ions, etc.

## 2. REFINED FITTING OF TETRAGONAL AND TRIGONAL GALLO-GERMANATE $^{57}Fe$ MÖSSBAUER SPECTRA

All  $^{57}Fe$  Mössbauer spectra of the tetragonal and trigonal Ca-gallo-germanate families show a notable large line-widths of resonances, both in paramagnetic and in magnetic ordering regions. In the paramagnetic phase the experimental values of the line-width are two or three times and in the magnetic ordering region overflow five or six times the natural one. That means several slight but different crystal fields, inducing energy split dispersion of the  $^{57}Fe$  nuclear levels. These splits are higher to half line-width of resonances. The results have been qualitatively explained by the effect of the random distribution of  $A^{2+}/Ln^{3+}$  in A (Thompson cube) and  $Fe^{3+}/Ge^{4+}$  Oh octahedrons and/or T tetrahedrons in the mentioned structures, in such crystalline media [8–14], taking into account the crystalline structural arguments and the XRD data [4–7]. That is considered as an effect of the static disorder.

Moreover, the deconvolution of spectra in more than two quadrupole or magnetic hyperfine sublattices and in consequence the dispersion of the hyperfine field values is suggested by the presumption that different crystalline fields are given by different number of tetra- and trivalent ions in the first cation surrounding the Mössbauer isotope.

In order to find the real crystal field dispersion in such structures, the experimental spectra were fitted with more refined soft.

In the paramagnetic region the spectra were refined by the  $\chi^2$  procedure in seven up to ten quadrupole doublets for Sr- Ba- and, respectively, Sr (Ln) trigonal germanate samples. In Fig. 1 is plotted the refined deconvolution of two experimental spectra.

In Table 1 the quadrupolar sublattices are arranged on the central shift and the decreasing values of the quadrupole splitting. The errors of the central shift,  $\varepsilon_8$  are

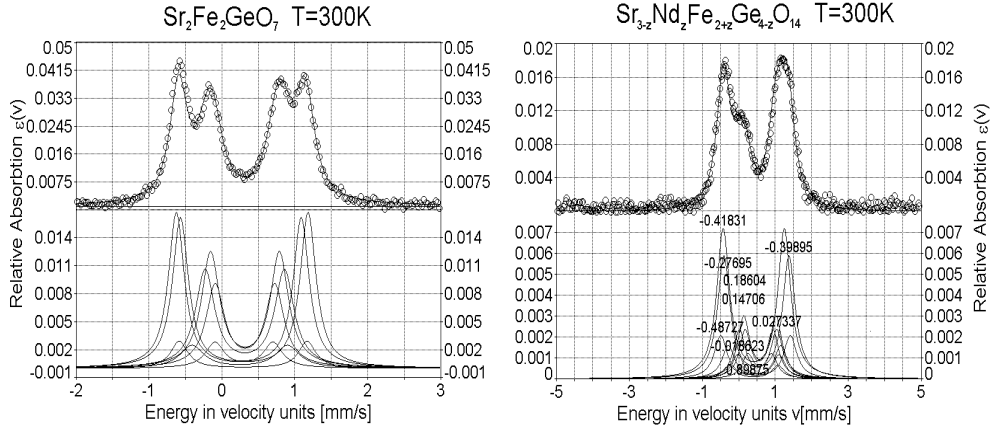


Fig. 1 – Deconvolution of the Sr-Ge ferrigehlenite and Sr (Nd) ferri-gallate room temperature spectra.

about equal with that of the line-width of resonances  $\varepsilon_T = \varepsilon_\delta$  and half of the quadrupole splitting one  $\varepsilon_{\Delta Q} = 2\varepsilon_\delta$ , for every sublattice. The error-level of sublattice  $i$  depends on the ratio  $1/a_i$ , so the low intense sublattice has a high level of errors. In these circumstances the highest values of the central shift errors are in the range  $\varepsilon_\delta \in [0.01 \div 0.1]$  mm/s. The observed errors of the sublattice areas are  $\varepsilon_a \in [1.7 \div 2.7]\%$ .

In the magnetic ordering region, the spectra were resolved taking into account the effect of the very closed transmission geometry and the high intensity of the source. So, a slow parabolic background was introduced in order to reach a refined deconvolution of the spectra.

At liquid helium temperature (LHeT), the Mössbauer spectra of the investigated samples are very complex. That suggests the presence of a large number of sublattices. The observed and fitted sublattices are listed in Table 2. They were grouped on the central shift and the increasing hyperfine magnetic fields. The low values of the quadrupole shifts can be explained by the critical values of the angle  $\vartheta$  between the electric gradient and the hyperfine magnetic field axes,  $\cos^2\vartheta = 1/3$ . In Fig. 2 are plotted the experimental and fitted LHeT spectra for the Sr and Sr (Nd) samples.

The refined deconvolution of the room temperature spectra show the presence of the electric gradient field dispersion at  $^{57}\text{Fe}$  located in the T1 and T2 sites and, respectively, in the Oh and T1 sites in the tetragonal and trigonal Ca-gallogemranate.

As in the case of the paramagnetic spectra, the refined deconvolution of the LHeT spectra shows the magnetic hyperfine field dispersion at the two sites occupied by Fe in such crystalline media.



One can observe that in the magnetic ordering region no dispersion of quadrupole shift  $\delta\Delta'$  can evaluate, due to its low values which are less or of the same order as the error limits.

Table 2

The hyperfine parameters of the  $^{57}\text{Fe}$  Mössbauer spectra in tetragonal ferrighelenite and trigonal ferri- and trivalent lanthanide-gallate at LHeT

Nr	Spectrum Parameters	Ba-Ge $r^2 = 0.82$	Sr-Ge $r^2 = 0.81$	Sr-Si $r^2 = 0.83$	Sr(La) $r^2 = 0.80$	Sr(Nd) $r^2 = 0.92$
1	$\delta_{Rh}$ [mm/s]	0.63	0.54	0.45	0.71	0.62
	$\varepsilon_Q$ [mm/s]	-0.21	-0.14	-0.13	0.16	0.36
	$H_{hf}$ [T]	31.00	32.23	31.85	44.43	43.10
	$a$ [%]	2.15	2.54	1.69	1.33	3.28
2	$\delta_{Rh}$ [mm/s]	0.63	0.54	0.45	0.66	0.61
	$\varepsilon_Q$ [mm/s]	-0.21	-0.15	-0.12	0.23	0.36
	$H_{hf}$ [T]	32.68	35.08	34.99	45.24	44.64
	$a$ [%]	9.94	10.88	7.32	4.59	7.59
3	$\delta_{Rh}$ [mm/s]	0.63	0.54	0.46	0.62	0.60
	$\varepsilon_Q$ [mm/s]	-0.21	-0.15	-0.12	0.25	0.36
	$H_{hf}$ [T]	34.7	37.52	37.71	46.17	45.65
	$a$ [%]	17.22	18.10	12.17	8.85	9.75
4	$\delta_{Rh}$ [mm/s]	0.63	0.54	0.45	0.62	0.60
	$\varepsilon_Q$ [mm/s]	-0.21	-0.15	-0.12	0.25	0.35
	$H_{hf}$ [T]	36.5	39.75	40.31	47.41	47.95
	$a$ [%]	13.26	13.40	8.97	9.10	4.39
5	$\delta_{Rh}$ [mm/s]	0.63	0.54	0.45	0.61	0.60
	$\varepsilon_Q$ [mm/s]	-0.21	-0.14	-0.12	0.24	0.34
	$H_{hf}$ [T]	38.13	41.67	42.70	49.10	49.00
	$a$ [%]	3.83	3.84	2.54	3.90	2.90
6	$\delta_{Rh}$ [mm/s]	0.44	0.25	0.27	0.45	0.54
	$\varepsilon_Q$ [mm/s]	0.11	0.24	0.40	0.51	0.08
	$H_{hf}$ [T]	23.87	29.50	29.00	33.10	36.30
	$a$ [%]	1.29	0.77	0.45	1.84	5.59
7	$\delta_{Rh}$ [mm/s]	0.44	0.25	0.26	0.46	0.54
	$\varepsilon_Q$ [mm/s]	0.11	0.24	0.41	0.54	0.08
	$H_{hf}$ [T]	27.35	31.13	30.84	36.09	38.44
	$a$ [%]	3.44	2.47	1.51	19.35	14.65
8	$\delta_{Rh}$ [mm/s]	0.44	0.25	0.27	0.48	0.54
	$\varepsilon_Q$ [mm/s]	0.11	0.24	0.39	0.54	0.08
	$H_{hf}$ [T]	30.08	32.87	32.99	41.19	40.49
	$a$ [%]	25.36	26.53	15.45	50.80	19.50
9	$\delta_{Rh}$ [mm/s]	0.44	0.25	0.27		0.534
	$\varepsilon_Q$ [mm/s]	0.11	0.24	0.41		0.08
	$H_{hf}$ [T]	35.00	35.50	35.70		42.52
	$a$ [%]	24.74	24.00	15.29		12.65

(continues)

Table 2 (continued)

Nr	Spectrum Parameters	Ba-Ge $r^2 = 0.82$	Sr-Ge $r^2 = 0.81$	Sr-Si $r^2 = 0.83$	Sr(La) $r^2 = 0.80$	Sr(Nd) $r^2 = 0.92$
10	$\delta_{Rh}$ [mm/s] $\varepsilon_Q$ [mm/s] $H_{hf}$ [T] $a$ [%]					0.54 0.07 44.61 4.76
ERRORS	$\delta_{Rh}$ [mm/s] $\varepsilon_Q$ [mm/s] $H_{hf}$ [T] $a$ [%]			0.006÷0.02 0.010÷0.04 0.2÷0.3 1.8÷2.7		

Finally from the experimental data, the experimental parameters of the crystal field dispersions were determined. The considered dispersion parameters are average values of the quadrupolar splitting  $\bar{\Delta}_Q$  and the magnetic hyperfine field  $\bar{H}_{hf}$  and their corresponding dispersion widths  $\delta\Delta_Q$  and  $\delta\Delta_H$ . The simple formulas were used to estimate the hyperfine field dispersion at the Mössbauer isotope.

$$\bar{\Delta} = \frac{\sum_i a_i \Delta_i}{\sum_i a_i}; \quad \delta\Delta = \mathbf{max}\{\Delta_i\} - \mathbf{min}\{\Delta_i\} \quad (1)$$

where  $\Delta_i$  are the hyperfine parameters of the hyperfine electric and magnetic interaction, which are determined by the refined analysis of the spectra. In Table 3 are given the experimental values of the dispersion parameter.

### 3. DISSCUSSION

#### 3.1. THE MELILITE STRUCTURE

The RT spectra of ferrighlenite with the highest iron content show up to eight quadrupolar doublets. That corresponds to the different crystalline surrounding around the Mössbauer isotope located in the crystal sites. The sublattices of every spectrum are divided into two groups, each of them having nearly but not exactly the same value as the central shifts. So, the first group contains the first five sublattices and the second one contains the last three sublattices of Table 1.

The quadrupole doublets of the both groups show small values of the central shift, due to the covalency effects.

The average values of the quadrupole splitting (Table 3), corresponding to each group, are very close to the obtained values of the rough deconvolution of the melilite spectra (see Table 4a of [1]). The first group is characterized by a smaller average value of the quadrupole splitting relatively to the second one. Taking into account the geometrical aspects, the quadrupole doublets of the first group were attributed to  $\text{Fe}^{3+}$  in T1 and, respectively, ed T2 sites. That is in agreement with the pervious Mössbauer study on  $\text{Fe}^{3+}$ -Ga melilite solid solution [15, 16]. One can remark that the total area of each group is very close to the values obtained in the previous deconvolution (see Table 4a in [1]). The occupancy of the T1 site is twice more than the T2 one.

Table 3

The values of the observed  $\bar{\Delta}$ ,  $\delta\Delta$  and Gaussian-fit dispersion  $x_o$ ,  $w$  parameters  $\bar{H}_{hf}$

Sample	Site	$\bar{\Delta}_Q$ [mm/s]	$\delta\Delta_Q^1$ [mm/s]	$x_Q$ [mm/s]	$w_Q^2$ [mm/s]	$\bar{H}_{hf}$ [T]	$\delta\Delta_H^3$ [T]	$x_H$ [T]	$w_H^4$ [T]	
Tetragonal ferri- gehlenites	Ba-Ge	T1	1.22	0.42	1.22	0.15	34.89	7.13	34.85	3.49
		T2	1.63	0.34	1.62	0.15	32.03	11.13	32.54	3.25
	Sr-Ge	T1	1.00	0.51	1.02	0.17	37.64	11.44	37.24	4.87
		T2	1.69	0.15	1.72	0.15	33.92	6.00	34.14	2.74
	Sr-Si	T1	0.97	0.40	1.02	0.26	37.90	11.15	37.50	2.70
		T2	1.70	0.10	1.63	0.21	34.11	6.70	34.40	1.50
Trigonal ferri- and trivalent lanthanide-gallate	Ba	Oh	0.93	0.40	0.91	0.23	–	–	–	–
		T1	1.80	0.56?	1.76	0.45	–	–	–	–
	Sr	Oh	0.96	0.40	0.95	0.24	–	–	–	–
		T1	1.75	0.43	1.67	0.42	–	–	–	–
	Sr(La)	Oh	0.94	0.65	0.91	0.34	46.87	4.67	47.30	2.33
		T1	1.73	0.48	1.70	0.31	39.33	7.91	39.50	4.07
	Sr(Nd)	Oh	0.92	0.72	0.91	0.30	45.78	5.90	44.50	2.51
		T1	1.68	0.57	1.61	0.26	40.34	8.31	40.01	3.93

<sup>1</sup> Observed data of  $\Delta$  at 300 K.

<sup>2</sup> Double Gaussian Fit of observed data  $a(\Delta)$  at 300 K.

<sup>3</sup> Observed data of  $H_{hf}$  at 4.2 K.

<sup>4</sup> Double Gaussian Fit of observed data  $a(H_{hf})$  at 4.2 K.

By the plot of the relative areas of the sublattices *versus* the experimental values of the quadrupole splitting, the dispersion of the electric field gradient in every investigated compound is shown.

The observed data were fitted by the multi-Gaussian peak function by the  $\chi^2$ -criterium procedure. In Table 3 are given the dispersion parameters, position and width of the two Gaussian components, corresponding to iron in the T1 and T2 sites. Fig. 3 contains the dispersion of the  $\Delta_Q$  values for Ba-Ge and Sr-Ge samples and their multiple Gaussian fit, as an example.

As one can see in Table 3, the two Gaussian components are very sensible to the sort of ion occupying the Thompson cube and the T2 sites. So the decrease of the ionic radius ( $\text{Ba}^{2+} \rightarrow \text{Sr}^{2+}$ ) in the Thompson cube induces the increase of the departure between the peaks and of the T1 component width. Moreover, the decrease of the ionic radius ( $\text{Ge}^{4+} \rightarrow \text{Si}^{4+}$ ) in the T2 sites induces a clear extent of the two component widths and a small decrease (in the error limits) of the distance between the peaks.

The LHeT spectra were fitted with nine magnetic sextets, which were divided into two groups taking into account the similar values of the central shift, assigned to  $\text{Fe}^{3+} : \text{T1}$  and  $\text{Fe}^{3+} : \text{T2}$ . The fitted parameters are given in Table 2. In Fig. 4 the magnetic hyperfine dispersion is plotted for the Sr-Ge and Sr (Nd) samples at LHeT. Taking into account the crystal chemistry of the melilite structure and the location of iron in such media, the group with the higher value of the central shift was designated to  $\text{Fe}^{3+} : \text{T1}$  and the second group, having the smaller value, to  $\text{Fe}^{3+} : \text{T2}$ . Generally, the higher values of  $\delta_{CS}$  at LHeT relatively to the RT spectra can be explained by the contribution of the second Doppler shift. The magnetic sublattices of each group characterize similar values of the quadrupole shift with the opposite sign. That denotes an opposite tetrahedral distortion and the angle between the magnetic hyperfine field and the main electric field gradient tensor axis is very close to  $\cos^2 \vartheta = 1/3$ .

A multi-Gaussian fit deconvolution of the experimental data is shown in Table 3. Firstly one can remark the higher value of the Gaussian widths in the magnetic ordering region relatively to the paramagnetic one,  $w_H \in [0.49 \div 1.55]$  mm/s,  $w_Q \in [0.15 \div 0.26]$  mm/s. That means a larger dispersion of the magnetic hyperfine fields with respect to the electric field gradient at the Mössbauer isotope position. The magnetic hyperfine field dispersion is more sensitive to the sort of ions in the A and T2 sites, relatively to the electric field gradient dispersion. So, the Gaussian components of the dispersion show the larger value for  $\text{Fe}^{3+} : \text{T1}$ ,  $w_H \in [0.86 \div 1.55]$  mm/s, and the smaller one for  $\text{Fe}^{3+} : \text{T2}$ ,  $w_H \in [0.49 \div 1.04]$  mm/s. The smaller value of the two Gaussian components is shown for the case of  $\text{Si}^{4+} : \text{T2}$  (ferrigehlenite of silicium). The greater value is given for Sr-Ge. The relative distance between the peak positions of the dispersion components is increased by the substitution of  $\text{Ba}^{2+}$  with  $\text{Sr}^{2+}$ , but it seems is not sensitive to  $\text{Ge}^{4+} \rightarrow \text{Si}^{4+}$ .

### 3.2. THE TRIGONAL GALLO-GERMANATE STRUCTURE

As in the case of the ferrigehlenite, the Mössbauer spectra of the iron-lanthanide trigonal gallogermante of Ba and Sr exhibit a convolution of many sublattices both in the paramagnetic range and in the magnetic one. The sublattices of the RT and LHeT spectra were grouped into two groups characterized by similar

values of the central shift for every sample. Generally the sublattices having the higher value of  $\delta_{CS}$  were considered in the first group and all the sublattices with the smaller one in the second group. The high values of the central shift denote a high ionicity of the ferric ion hosting the Mössbauer isotope and a high coordination around it. The mean value of the quadrupole splitting  $\bar{\Delta}_Q$  corresponding to the two groups is larger for the second group and smaller for the first one. Taking into account the crystal structure of the trigonal-germanate and the possible location of the ferric ions, all the above-mentioned observations suggest to designate the quadrupole doublets of the first groups to  $\text{Fe}^{3+} : \text{Oh}$  and to  $\text{Fe}^{3+} : \text{T1}$  for the sublattices of the second group.

The plots of the relative areas *versus* the quadrupole splitting and magnetic hyperfine fields evidence the dispersions of the crystal fields at each of the sites occupied by the Mössbauer isotope (see Figs. 3 and 4 for simple examples). Two components were separated in the crystal field dispersion by the multi-Gaussian fit. Those components correspond to the crystal field dispersions by the iron in Oh- and T1 sites.

The dispersion of the crystal fields is very sensitive to the sort of ion located in the A- Oh- and T1 site in the trigonal germanate structure. So in the paramagnetic range, the substitution of alkaline-earth metals by lanthanide ions determines an increase of the Gaussian component's widths. The increasing rate is higher for the crystal field dispersion by the  $\text{Fe}^{3+} : \text{Oh}$  site. Moreover the decrease of the lanthanide ionic radius determines an extension of the Gaussian component's widths. A similar feature is in the magnetic ordering region too, but one can remark that the iron trigonal gall-germanate without the lanthanide ions in the Thompson cube site at LHeT evidences an unsaturated magnetic ordering for the Ba sample and none for the Sr sample. The low abundance of the magnetic ions and the small value of the superexchange interaction energy in such crystalline media can explain that. Also one can point out the similar values of the Gaussian component's widths in the para- and magnetic ordering range.

The similar evolution of the crystal field dispersion of  $\text{Fe}^{3+} : \text{T1}$  in the melilite structure and of  $\text{Fe}^{3+} : \text{Oh}$  in the Ca-gallate one can be a proof to consider the two structures linked by profound structural phase transformation. That is in agreement with the supposition of two origins of the T1 tetrahedrons in the trigonal gallogermante. Indeed, as was shown in [4, 17], comparing the trigonal and the tetragonal structures, the former can be constructed like the tetragonal one by a similar unit cell. In this manner, it seems evident that one of the T1 tetrahedrons can be considered as proceeding from the T2 one, which, because of the formation of the octahedron, breaks the five member ring, turns and takes position on the  $L_2$  axis. The second origin is from the T1 tetrahedrons of the melilite structure.

#### 4. CONCLUSIONS

The tetragonal and trigonal ferrigehlenites, having extreme iron content, are the typical static disordered crystalline media. These crystalline media are known as hosting the structure of the tunable solid laser. The refined analysis of their RT and LHeT Mössbauer spectra showed a convolution of the electric or magnetic crystal field dispersion curves, corresponding to each of two sites located by the Mössbauer isotope.

The dispersion curves were fitted by a multi-Gaussian function. Generally in the case of the melilite structure, the width of the Gaussian component is smaller for the paramagnetic range and greater in the magnetic ordering region. In the case of the Ca-gallate structure the widths have approximately the same values.

Both in the paramagnetic range and in the magnetic ordering region, the two Gaussian components of the crystal fields' dispersion superpose for both the investigated structures. But one can observe a strong dependence of the superposition degree on the sort of the substituting ions in the Thomson cube and the tetrahedral sites.

The higher Gaussian widths are shown for the  $\text{Fe}^{3+}$  : T1 and  $\text{Fe}^{3+}$  : Oh site in the melilite and, respectively, Ca-gallate structure. The Gaussian dispersion of the crystal fields at  $^{57}\text{Fe}$  is very sensitive to the change of the ionic sort and its concentration in the surrounding positions. So, the ions with smaller volume and higher ionicity and located in the Thomson cube ( $\text{Ba}^{2+} \rightarrow \text{Sr}^{2+} \rightarrow \langle \text{Sr}^{2+}, \text{La}^{3+} \rangle \rightarrow \langle \text{Sr}^{2+}, \text{Nd}^{3+} \rangle$ ) and in the T2 tetrahedrons ( $\text{Ge}^{4+} \rightarrow \text{Si}^{4+}$ ) generate an extension of each Gaussian component and an increase of the distance between their peak positions.

The results obtained by the investigations of these static-disorder crystalline media can suggest the preferable location of the laser ions in such media. Supposing a direct dependence between the dispersion width of the crystal field and the broad-band tunable selected emission from laser activators ( $\text{Ln}^{3+}$ ,  $\text{Cr}^{3+}$ , etc.) in such crystalline media, their investigation shows the possibility to vary the tunable range by the above-mentioned ionic substitution.

*Acknowledgement.* The author expresses his gratitude to:

- the MEC "CERES" National Research Program project 14/15.10.2001, "*Investigarea non distructivă și modelarea numerică a geometriei, dinamicii locale și a proprietăților electro-magneto-optice în micro- și nano-structuri cristaline static-dezordonate 2001–2004*", for the financial support to carry out the Mössbauer measurements and the possibilities to accede to powerful computing machines;
- the *Deutsche Forschungsgemeinschaft*, the *European Science Foundation* ("MOLECULAR MAGNETS" Program) and UNIVERSITY OF MAINZ, for the financial support to present the obtained results at 5th Seeheim Workshop on Mössbauer Spectroscopy, Germany, May, 21–26, 2002.
- Professors *I. S. Lyubutin* from I.K.A.N., Moscow, and *P. Gutlich* from the University of Mainz, for scientific advice and support.

## REFERENCES

1. S. Constantinescu, *Rom. Journ. Phys.* **47**, 5–6, I (2003).
2. S. Constantinescu, *Rom. Journ. Phys.* **47**, 5–6, II (2003).
3. S. Constantinescu, 5th Seeheim Workshop on Mössbauer Spectroscopy, May 21–25, 2002, Seeheim, Germany, P15.
4. E. L. Belokoneva and N. V. Belov, *Dokl. Ross. Ak. Nauk* **260**, 1363 (1981).
5. E. L. Belokoneva, N. A. Simeonov, A. V. Butashin, B.V. Mill and N. V. Belov, *Dokl. Ross. Ak. Nauk* **255**, 1099 (1980).
6. A. V. Butashin, B. V. Mill, G. G. Khodzhabagyan, E. L. Belokoneva and N. V. Belov, *Dokl. Ross. Ak. Nauk* **264**, 1385 (1982).
7. A. A. Kaminskii, *Phys. Status Sol.* **86**, 1 345 (1985).
8. I. S. Lyubutin, B. V. Mill, V.G. Terziev, A. V. Butashin, *Kristallogr.* **33**, 136 (1988).
9. D. Barb, S. Constantinescu, D. Tarina, I. S. Lyubutin, B. V. Mill, V. G. Terziev, T. V. Dmitrieva, A. V. Butashin, *Rev. Roum. Phys.* **33**, 1111 (1988).
10. D. Barb, S. Constantinescu, D. Tarina, I. S. Lyubutin, B. V. Mill, V. G. Terziev, T. V. Dmitrieva, A. V. Butashin, *Hyperfine Interactions* **50**, 645 (1989).
11. D. Barb, S. Constantinescu, D. Tarina, I. S. Lyubutin, B. V. Mill, V. G. Terziev, T. V. Dmitrieva, A. V. Butashin, *Proc. 1st General Conference. of the Balkan Physics Union*, Sept. 26–28, 1991, Thessaloniki, Greece, p. 808–810.
12. D. Barb, S. Constantinescu, D. Tarina, I. S. Lyubutin, V. G. Terziev, T. V. Dmitrieva, 26th Congress Ampere on Magnetic Resonance, 1992, Athens, Greece, p. 496–497.
13. D. Barb, S. Constantinescu, D. Tarina, *Hyperfine Interactions* **96**, 73 (1995).
14. D. Barb, S. Constantinescu, D. Tarina, *Hyperfine Interactions* **96**, 83 (1995).
15. M. Akasaka and H. Ohashi, *Phys. Chem. Miner.*, **12**, 13, (1985).
16. M. Akasaka and H. Ohashi, *Phys. Chem. Miner.*, **13**, 152 (1986).
17. B. Barb, S. Constantinescu D. Tarina, *Rev. Roum. Phys.* **38**, 1, 95 (1993).